Journal of Power Sources 184 (2008) 562–565

Contents lists available at ScienceDirect

Journal of Power Sources

journal homepage: www.elsevier.com/locate/jpowsour

Short communication

Macroporous nanocomposite polymer electrolyte for lithium-ion batteries

Z.H. Li[a,b,c], H.P. Zhang[a], P. Zhang[a], Y.P. Wu[a,*], X.D. Zhou[c]

[a] Department of Chemistry & Shanghai Key Laboratory of Molecular Catalysis and Innovative Materials, Fudan University, Shanghai 200433, China
[b] College of Chemistry, Xiangtan University, Hunan 411105, China
[c] State Key Laboratory of Chemical Engineering, East China University of Science and Technology, Shanghai 200237, China

ARTICLE INFO

Article history:
Received 4 January 2008
Received in revised form 5 February 2008
Accepted 13 February 2008
Available online 29 February 2008

Keywords:
Nanocomposite polymer electrolyte
P(VDF-HFP)
Macroporous polymer membrane
Ionic conductivity
Lithium-ion battery

ABSTRACT

A novel macroporous nanocomposite polymer membrane (NCPM) based on poly(vinylidene difluoride-co-hexafluoropropylene) [P(VDF-HFP)] copolymer was prepared by *in situ* hydrolysis of $Ti(OC_4H_9)_4$ using a non-solvent-induced phase separation technique. SEM micrograph shows that the yielding TiO_2 nanoparticles are dispersed uniformly in the polymer matrix and there are a lot of spherical macropores connecting with each other by some smaller pores. DSC results exhibit that the crystallinity of polymer matrix decreases with the incorporation of TiO_2 nanoparticles. The tensile stress of the NCPM is 9.69 MPa and its fracture strain 74.4%. After immersion in 1.0 mol l^{-1} $LiPF_6$/ethyl carbonate (EC)–dimethyl carbonate (DMC), the ionic conductivity of the obtained nanocomposite polymer electrolyte (NCPE) is 0.98×10^{-3} S cm^{-1} at 20 °C. Lithium-ion batteries, which use this kind of NCPE as the separator and electrolyte, display good discharging performance at different current densities, presenting promise for its practical application.

1. Introduction

Gel polymer electrolyte (GPE) based on poly(vinylidene difluoride-co-hexafluoropropylene) copolymer [P(VDF-HFP)] has been widely studied since the first disclosure in 1994 [1]. Because P(VDF-HFP) cannot dissolve in carbonates, which are usually used as organic solvents of non-aqueous electrolyte for lithium secondary batteries, it acts as a supporting backbone in GPE to improve its physical property. In addition, nanoscale ceramic powders such as Al_2O_3, $LiAlO_2$, SiO_2, TiO_2 and molecular sieves were added directly into GPE to enhance its mechanical strength and ionic conductivity [2–13]. However, nanoparticles aggregate easily within polymer matrix on account of their high surface energy during the formation of polymer membranes. Many technologies have been applied to inhibit the aggregation of nanoparticles, for example, modification of the surface of nanoparticles, sol–gel technology, *in situ* polymerization and formation [14–22]. Although high porosity of polymer membranes leads to high ionic conductivity, their mechanical properties will be traded-off. As separator for polymer lithium-ion batteries (PLiBs), the porous gel polymer electrolyte (PGPE) should guarantee not only high conductivity but also good mechanical properties.

Here we chose $Ti(OC_4H_9)_4$ as the precursor of TiO_2 nanoparticles and make it hydrolyze *in situ* in a polymer solution. The hydrolyzed nanoparticles dope into the polymer matrix *in situ* to produce the nanocomposite polymer membranes (NCPMs). The obtained NCPMs are dimensionally stable and flexible in favor of continuous industry production. They display good electrochemical properties, which are promising for practical application.

2. Experimental

0.96 g of $Ti(OC_4H_9)_4$ was dissolved in 9.0 g 10 wt.% solution of P(VDF-HFP) powder (Kynar® 2801) in a mixed solvent consisting of *N*-methyl pyrrolidone (NMP) and *n*-butyl alcohol (C_4H_9OH) (the volume ratio of NMP to C_4H_9OH is 8:1). To avoid the drastic hydrolysis of the precursor, a little of concentrated hydrochloric acid was dropped into the polymer solution to adjust its pH to about 1.0 before. Then the mixture was cast on the glass plate and then dried at 80 °C for 4 h. The nanocomposite polymer membranes were finally obtained by immersed in water at 80 °C for 2 h.

The mass fraction of TiO_2 coming from *in situ* hydrolysis of $Ti(OC_4H_9)_4$ in NCPM was determined by TGA under air atmosphere heated up to 800 °C at a rate of 20 °C min^{-1}. Their micrographs were taken by Philips XL30 scanning electron microscope. The crystal structure of NCPMs was measured by Bruker D8 X-ray diffraction instrument. The mechanical measurement of NCPMs was carried out with Zwick 20TN2S apparatus, at a crosshead speed of 5 mm min^{-1}, using a mini-tensile bar with length 2.40 cm, thickness 0.060 cm and width 0.45 cm. The tests were carried out at room temperature.

* Corresponding author. Tel.: +86 21 55664223; fax: +86 21 55664223.
E-mail address: wuyp@fudan.edu.cn (Y.P. Wu).

0378-7753/$ – see front matter © 2008 Elsevier B.V. All rights reserved.
doi:10.1016/j.jpowsour.2008.02.068

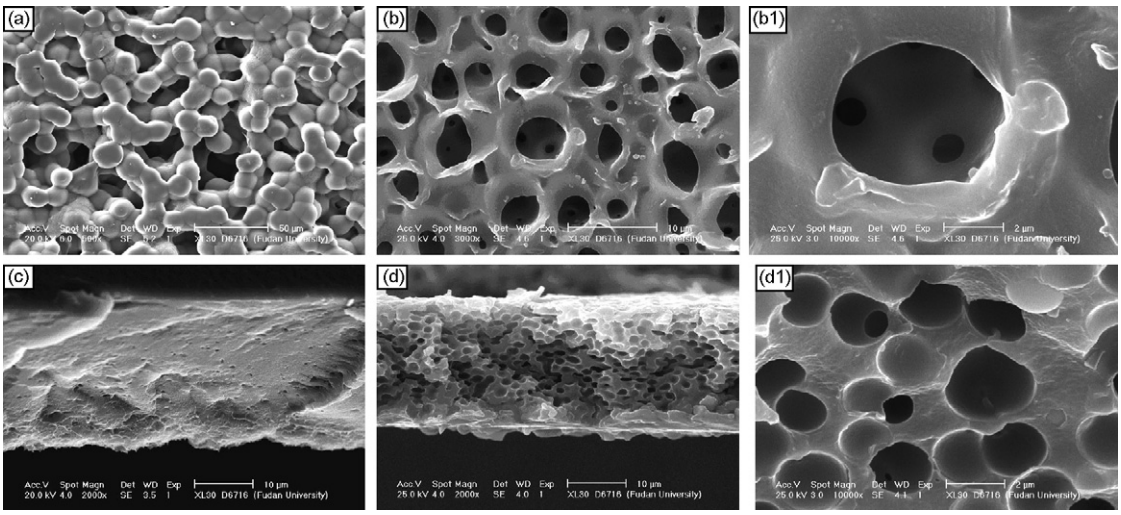

Fig. 1. Micrographs of polymer membranes: (a) surface of the pure polymer membrane, (b) surface of the NCPM, (b1) amplificatory micrograph of (b), (c) cross-section of the pure polymer membrane, (d) cross-section of the NCPM and (d1) amplificatory micrograph of (d).

The electrolyte uptake of polymer membrane was calculated by Eq. (1):

$$\text{Electrolyte uptake} = \frac{W_f - W_0}{W_0} \quad (1)$$

where W_0 is the net weight of polymer membrane, and W_f is the weight of the membrane after absorbing the liquid electrolyte.

The nanocomposite polymer electrolyte (NCPE) was obtained by impregnating the NCPM in liquid electrolyte of 1 M $LiPF_6$/ethyl carbonate (EC)–dimethyl carbonate (DMC) (w/w, 1:1) for 2 h. Its conductivity (σ) was calculated from the equation $\sigma = d/(R_b \times S)$ according to the Nyquist curves measured by electrochemical impedance spectroscopy on EG&G 273 electrochemical analysis system where d, S and R_b are thickness, area and bulk resistance of polymer electrolyte, respectively. Polymer lithium-ion batteries were manufactured by sandwiching the NCPE between $LiCo_{1/3}Ni_{1/3}Mn_{1/3}O_2$ positive electrode and CMS negative electrode and sealed in a model cell in a glove-box.

3. Results and discussion

Fig. 1 shows the micrographs of the surface and cross-section of polymer membranes. As to the pure polymer membrane, many connected spherical crystals formed a little amount of irregular pores (Fig. 1a), and the polymer matrix looks very compact (Fig. 1c). Fig. 1b shows that many spherical macropores with a diameter of about 5 μm appeared on the surface of NCPM and interconnected through some smaller pores like "windows". The NCPM has a porous structure as shown in Fig. 1d. The hydrolyzed TiO_2 nanoparticles dispersed uniformly in polymer matrix as shown in the amplified micrographs (Fig. 1b1 and d1). The uptake ratio of electrolyte for polymer membranes was depicted in Table 1. The electrolyte uptake ratio of the NCPM is 125%, larger than that of the pure polymer membrane by 56%, due to much more macropores.

Fig. 2 shows that the characteristic peaks of the P(VDF-HFP) crystals are situated at 18.02° (020, β), 20.41° (110, β) and 36.09° (200, α), respectively. The intensities of these peaks decrease slightly after the doping of TiO_2 into the polymer matrix while their positions are basically unchanged, indicating that the crystal structure of the polymer matrix does not change with the incorporation of the TiO_2 nanoparticles. The characteristic diffraction peaks of rutile or anatase of TiO_2 were not observed, indicating that the formed TiO_2 is non-crystalline, and the new wide peak around 12.50° may be ascribed to the incorporated TiO_2 nanoparticles. The mass fraction of TiO_2 in NCPM was measured to be 9 wt.% by TGA.

Fig. 3 shows the DSC curves of the polymer membranes. The data of crystal fusion temperature (T_m), crystallization temperature (T_c),

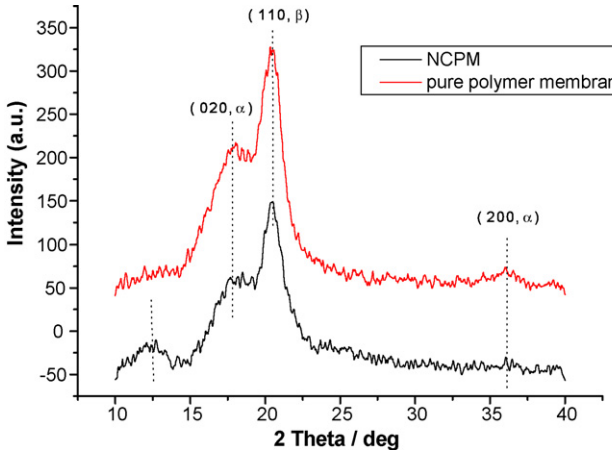

Fig. 2. XRD patterns of polymer membranes.

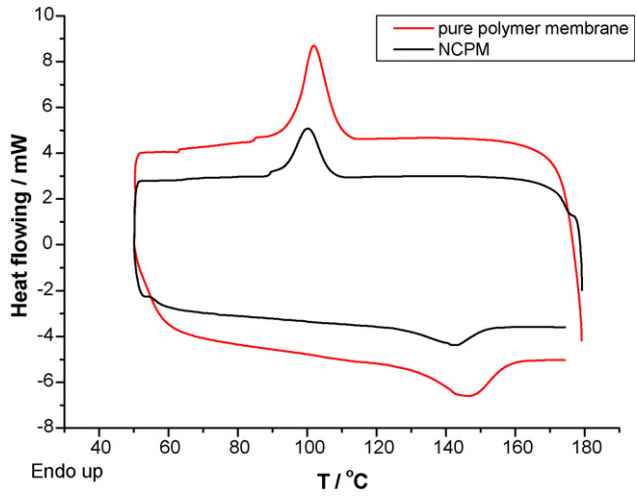

Fig. 3. DSC curves of polymer membranes.

Table 1
DSC data and electrolyte uptake ratio of polymer membranes

Materials	T_c (°C)	ΔH_c (J g^{-1})	T_m (°C)	ΔH_m (J g^{-1})	Electrolyte uptake ratio (%)
Pure polymer membrane	101.9	25.27	146.6	19.00	69
NCPM	100.1	21.57	142.2	14.27	125

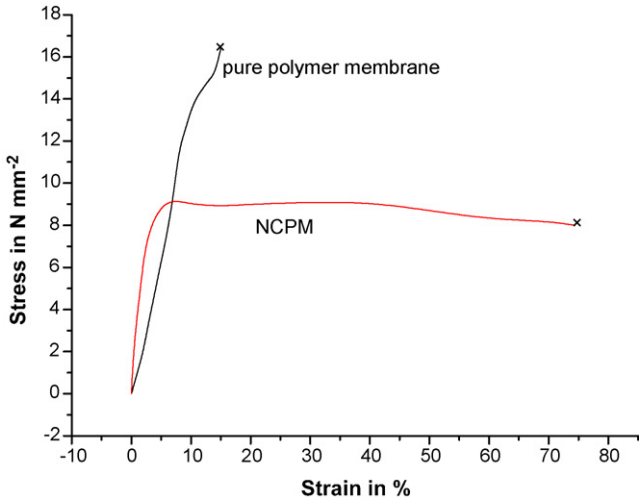

Fig. 4. Stress–strain curves for polymer membranes.

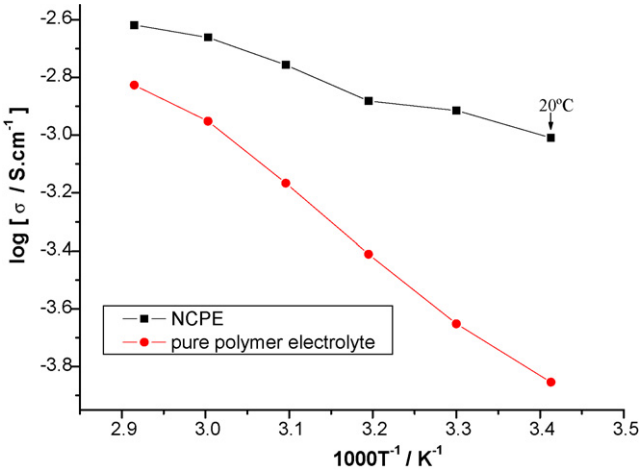

Fig. 5. $\log\sigma \sim 1/T$ curves for polymer electrolytes.

heat of crystal fusion (ΔH_m), and heat of crystallization (ΔH_c) are listed in Table 1. The T_m of NCPM is lower than that of the pure polymer membrane by 4.4 °C, and the heat of crystal fusion decreases by 4.7 J g^{-1}. The similar change was also observed during the crystallization process. The *in situ* formed nanoparticles become the knots of the re-crystallization of polymer molecular chains and thus the polymer molecular chains are disarranged, resulting in the decrease of the crystal fusion temperature and heat of crystal fusion of the polymer matrix.

Fig. 4 shows the stress–strain curves of the polymer membranes. The maximum stress of the pure polymer membrane is 16.40 MPa while that of NCPMs falls to 9.69 MPa. Nevertheless the fracture strain of the NCPMs (74.4%) is larger than that of the pure polymer membrane (15.0%) by 59.4%. On one hand, as there are a large amount of interfacial layers between nanoparticles and polymer matrix, the deformation of them will use up partial energy during stretching. On the other hand, the rest energy will be consumed by the deformation of macropores within polymer matrix. The pure polymer membrane is fragile whereas the NCPMs is flexile. It suggests that the NCPMs have a good property of elongation, benefiting to fabricate polymer lithium-ion batteries.

Fig. 5 shows the dependence of ionic conductivity on temperature ranging from 20 to 70 °C for the gel polymer electrolytes. It exhibits that the ionic conductivity of the gel polymer electrolyte made of the pure polymer membrane is 0.14×10^{-3} S cm^{-1} at 20 °C while that of the NCPE is 0.98×10^{-3} S cm^{-1}. It is well known that porous gel polymer electrolyte consists of three phases: the absorbed liquid electrolyte, the swollen gel polymer and the polymer matrix. On one hand, the electrolyte uptake of the NCPM is higher than that of the pure polymer membrane as shown in Table 1. On the other hand, much more inter-connected smaller pores facilitate the mobility of lithium ions. The former change brings about an increase of the number of lithium ions while the latter change leads to an increase of the transport channels. Besides that, the Lewis acid –OH groups on the surface of TiO_2 nanoparticles decrease the polarity of $-CF_2$ groups of polymer chains. Consequently, the interaction between Li^+ ions and $-CF_2$ groups is very weak [23]. All of these changes are contributed to the enhancement of the ionic conductivity for NCPE.

Fig. 6 shows the discharging specific capacity of PLiBs at different current densities where the NCPMs were used as a separator and electrolyte, the cathode ($LiCo_{1/3}Ni_{1/3}Mn_{1/3}O_2$) can deliver a discharge capacity of 145, 142 and 138 mAh g^{-1} at current density of 0.1, 0.2 and 0.5 mA cm^{-2}, respectively. In contrast, $LiCo_{1/3}Ni_{1/3}Mn_{1/3}O_2$ delivered a discharge capacity of 136, 127, and 120 mAh g^{-1}, respectively, if the pure polymer membrane was used as the separator. At 1.0 mA cm^{-2}, $LiCo_{1/3}Ni_{1/3}Mn_{1/3}O_2$ presented reversible capacity of about 120 and 100 mAh g^{-1}, respectively, when the NCPMs and the pure polymer membrane were used. The difference in the discharge capacity is due to higher electrochemical polarization resistance from the pure polymer membrane than the NCPMs. Since this kind of NCPM consists of macropores, which are filled with the liquid electrolyte, the conductivity will not change much with cycle number though a kind of slight decrease would be observed since a small amount of liquid electrolyte would be consumed to form a SEI film on the anode. It suggests that PLiBs using

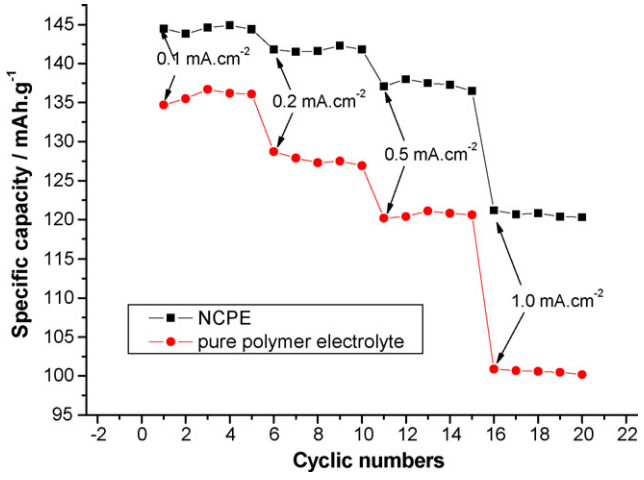

Fig. 6. Discharging capacity of PLiBs at different current densities.

this kind of NCPE as the separator and electrolyte are suitable to work at moderate current density.

4. Conclusion

The nanocomposite polymer membranes, which possess interconnected macropores through some smaller pores, have been successfully prepared by *in situ* hydrolysis of $Ti(OC_4H_9)_4$ in the solution of P(VDF-HFP) copolymer. Compared with the pure polymer membranes, the NCPMs can uptake much more non-aqueous electrolyte up to 125%. The NCPMs exhibit flexile structure with an elongation ratio of 74.4%. The ionic conductivity of the resulting NCPE is 0.98×10^{-3} S cm^{-1} at 20 °C. Polymer lithium-ion batteries using this kind of NCPE as the separator and electrolyte display good discharge performance, suggesting good promise for its practical application.

Acknowledgements

All of supporting from National Basic Research Program of China (973 Program No: 2007CB209700), China Postdoctrol Science Fund (20060400618), Hunan Natural Science foundation (06JJ4093), the Open Fund from State Key Laboratory of Chemical Engineering in East China University of Science and Technology (HF06008), and the Doctor Starting Fund from Xiangtan University (05QDZ18) are greatly appreciated.

References

[1] A.S. Gozdz, C.N. Schmutz, J.M. Tarascon, US Patent 5,296,138 (1994).
[2] H.P. Zhang, P. Zhang, Z.H. Li, M. Sun, Y.P. Wu, H.Q. Wu, Electrochem. Commun. 9 (2007) 1700.
[3] Z.H. Li, G.Y. Su, X. Wang, D.S. Gao, Solid State Ionics 176 (2005) 1903.
[4] N.T.K. Sundaram, A. Subramania, Electrochim. Acta 15 (2007) 4987.
[5] J.D. Jeon, M.J. Kim, S.Y. Kwak, J. Power Sources 162 (2006) 1304.
[6] K.M. Kim, N.G. Park, K.S. Ryu, S.H. Chang, Electrochim. Acta 51 (2006) 5636.
[7] Z.H. Li, H.P. Zhang, P. Zhang, Y.P. Wu, X.D. Zhou, Polym. Adv. Technol., in press.
[8] M.K. Wang, F. Zhao, Z.H. Guo, S.J. Dong, Electrochim. Acta 49 (2004) 3595.
[9] Y.X. Jiang, Z.F. Chen, Q.C. Zhuang, J.M. Xu, Q.F. Dong, L. Huang, S.G. Sun, J. Power Sources 160 (2006) 1320.
[10] M. Caillon-Caravanier, B. Claude-Montigny, D. Lemordant, G. Bosser, J. Power Sources 107 (2002) 125.
[11] D. Saikia, A. Kumar, Eur. Polym. J. 41 (2005) 563.
[12] C.G. Wu, M.I. Lu, C.C. Tsai, H.J. Chuang, J. Power Sources 159 (2006) 295.
[13] A.M. Stephan, K.S. Nahm, T.P. Kumar, M.A. Kulandainathan, G. Ravi, J. Wilson, J. Power Sources 159 (2006) 1316.
[14] X.M. He, Q.S. Shi, X. Zhou, C.R. Wan, C.Y. Jiang, Electrochim. Acta 51 (2005) 1069.
[15] Y.J. Wang, D. Kim, Electrochim. Acta 52 (2007) 3181.
[16] W.D. Lee, S.S. Im, J. Polym. Sci. B: Polym. Phys. 45 (2007) 28.
[17] C.S. Wu, J. Polym. Sci. A: Polym. Chem. 43 (2005) 1690.
[18] A. Akelah, A. Rehab, T. Agag, M. Betiha, J. Appl. Polym. Sci. 103 (2007) 3739.
[19] M. Avella, M.E. Errico, E. Martuscelli, Nano Lett. 1 (2001) 213.
[20] C. Bartholome, E. Beyou, E. Bourgeat-Lami, P. Chaumont, F. Lefebvre, N. Zydowicz, Macromolecular 38 (2005) 1099.
[21] Y.A. Shchipunov, T.Y. Karpenko, Langmuir 20 (2004) 3882.
[22] M. Watanabe, T. Tamai, Langmuir 23 (2007) 3062.
[23] Z.H. Li, H.P. Zhang, P. Zhang, Y.P. Wu, J. Appl. Electrochem. 38 (2008) 109.